

Navigation of Welding Torch for Arc Welding Process ^{*}

WeiJie Zhang, Jun Xiao, YuMing Zhang^{*}

^{} Electrical and Computer Engineering Department and Institute of Sustainable Manufacturing, University of Kentucky, Lexington, KY, 40508, USA (e-mail: weijie.zhang@uky.edu, jun.xiao@uky.edu, ymzhang@engr.uky.edu).*

Abstract: Torch position, traveling speed, and attitude play an important role in welding quality control for both manual and robotic arc welding process. Besides, their detection may facilitate welding process monitoring, welder training, as well as novel ways for many other interesting and useful applications. Yet, few research has been done in the torch navigation in manual arc welding process. In this paper, we describe and implement a Kalman-based framework to estimate the position, traveling speed, and attitude of a torch in manual welding process. The proposed framework makes use of an inertial navigation system (INS) mechanization algorithm, a Zero Velocity Update (ZUPT) methodology, and a unscented Kalman filter (UKF). The proposed measurement employs a low-price miniature wireless inertial measuring unit (WIMU) consisting of a tri-axial accelerometer, one tri-axial gyroscope and a magnetometer. The performance of the proposed scheme has been evaluated by welding simulations with different types of fit-ups. Statistics shows that the position errors are about 1% of the total traveled distance, which are considered acceptable for the intended manual welding applications.

Keywords: Torch position measurement, unscented Kalman filter, Inertial navigation, Zero velocity update, Manual welding.

1. INTRODUCTION

Arc welding has been developed and refined for years as one of the most widely used material joining/fabrication technology. The position, traveling speed and attitude of the torch are critical parameters which directly determines weld quality. Desirable welds can only be guaranteed if the torch is also properly controlled. Inappropriate torch manipulations cause various weld defects/discontinuities, such as poor penetration, undercut, porosity, and different types of cracks (Raj et al. (2002)-Moreno (2013)). Thereby, detailed torch manipulations for almost every welding process have been specified/recommended by both standardization organizations such as American Welding Society (AWS) (AWS (2003), AWS (2004)) and by different welding-related companies (Lin (1997), ESA (2011), MIL (2003)).

In robotic welding, the torch is moved by a welding robot such that the torch navigation parameters (attitude, traveling speed, and position) are taught and programmed. However, the teaching process is tedious and not time efficient for customized, small batch work pieces. A new teaching strategy can be developed using the proposed methodology: an experienced welder holds a torch with a rigidly mounted IMU to move along the target work piece as if it were in a real welding process. The navigation parameters, detected by the proposed methodology, can be

directly utilized in robot weld path teaching the process of which can be thus significantly simplified.

In manual arc welding, a welder cannot master torch adjusting maneuver without countless hours of practice, which makes the welder training cycle intolerably long. The torch navigation parameters can accelerate the welding training process: A database of welding experts' performance can be established using those parameters with other critical welding parameters. Using the database, the operations of a welding trainee can be compared with the expert's performance throughout the practice in real-time, and the incorrect/unfavorable torch operations can be identify immediately. Audio or visual indications thus can be provided as the instant performance feedback throughout the training practice (Vrt (2012), Teeravarunyou and Poopatb (2009)).

An inertial measuring unit (IMU) normally contains several accelerometers, gyroscopes, and magnetometers. The size and performance of an IMU are typically linearly dependent: the smaller the sensor the lower performance is expected. Microelectromechanical system based on IMUs are popular, yet they have a significant bias, and thus accumulate large drifts after integration.

Within the scope of our limited search capability, no literature has been found for the measurement of torch's attitude, traveling speed or position. In this paper, we describe and implement a Kalman-based framework to estimate the torch's navigation parameters (section III).

^{*} Sponsored by National Science Foundation under grant CMMI-0927707

The magnetometer and the Zero Angular Rate Update (ZARU) algorithm are integrated into the Kalman-based framework to reduce the sensor drift (section IV). Finally, the extended algorithm is tested in several welding simulations (section V).

2. EXPERIMENTAL SYSTEM

The IMU (Shimmer 9DOF motion sensor: 53mm × 32mm × 19mm) used in this study is shown in Fig. 1. The calibration procedure for the sensors is performed according to literature Ferraris et al. (1995). ${}^t(XYZ)$ and ${}^s(XYZ)$ denote the 3-D Cartesian coordinate systems for the torch and the WIMU, respectively. Axis tZ coincides with the torch head direction, axis tX coincides with axis sX . Frame ${}^t(XYZ)$ can be obtained by rotating frame ${}^s(XYZ)$ around sX axis for an angle, denoted as θ_{st} .

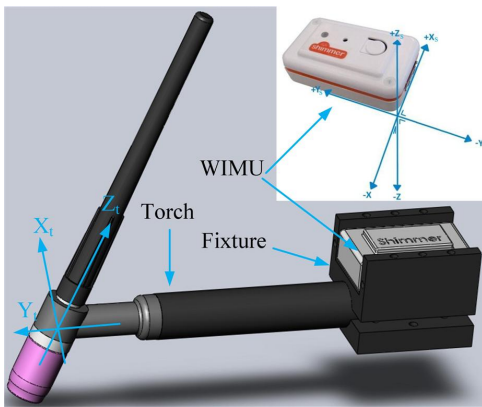


Fig. 1. The illustration of torch. The WIMU which is rigidly mounted on the torch handle.

3. THE KALMAN-BASED METHOD

3.1 Inertial Navigation System (INS)

The navigation parameters of the torch (in Fig. 1) can be calculated using data from the WIMU, i.e., the position and orientation estimation can be performed using double integration of the accelerometer data and integration of angular rate measurements from the gyroscope. Fig. 2 shows the INS process.

3.2 Quaternion based Kalman filter

One can find in Fig. 2 any errors in the initial alignment or the integration blocks will propagate over time. Thus, a self-correction mechanism is required in to order to accurate estimation in the INS. Most of the literature for INS modeling assumes that all perturbation attitude angle errors are small. However, in many cases this assumption does not hold. A Kalman filter mechanism was introduced to the INS in 1992 (Pham (1992)). This approach used non-linear variables to describe a heading angle, while the attitude errors were uncontrolled. The extended Kalman filter (EKF) is the most widely used approach for non-linear filter algorithms (Luongo and Veltink (2005), Luongo and Veltink (2004), Lee and Jung (2009), Schepers et al. (2010)). However, the implementation difficulty of Jacobians, used to expand the EKF models, is one major

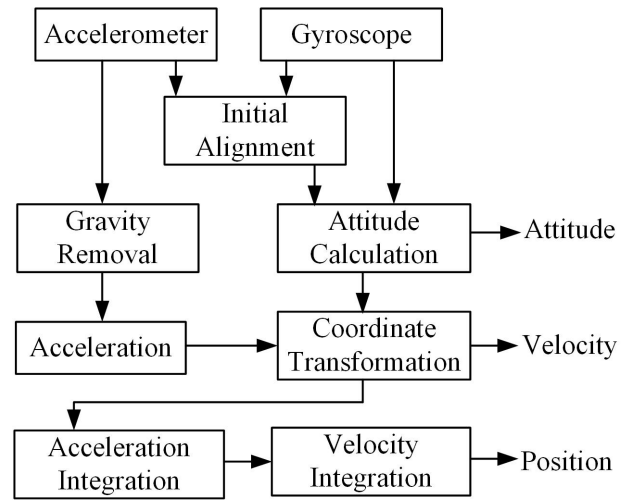


Fig. 2. INS process

shortcoming of the EKF. In this paper, the unscented Kalman filter (UKF) is implemented for the INS algorithm. An INS may compute the attitude using Euler angles, the direction cosine matrix or the quaternions. In this paper, the quaternion method is chosen since it requires less computation, gives better accuracy and avoids singularity (Chou (1992)). Figure 3 shows the main blocks in the proposed Kalman-based framework for the torch navigation.

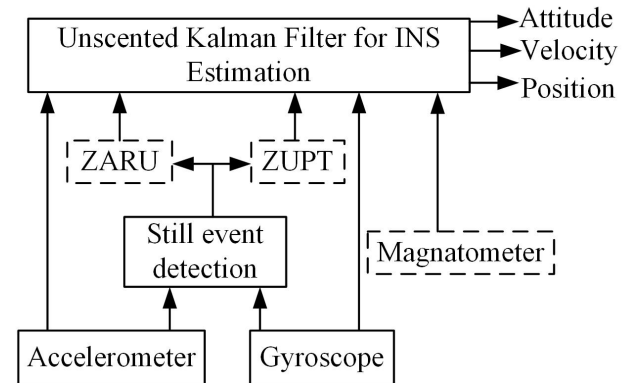


Fig. 3. The Kalman-based framework use for torch navigation: An unscented Kalman filter that estimates the navigation parameters related to the INS; a Zero-Velocity-Update (ZUPT) block that feeds the UKF with measurement to correct the velocity bias.

The accelerometer and gyroscope reading, in the sensor body (s) frame of reference, (a_k^s and w_k^s , respectively) are taken every sample interval T_s at discrete sampling time k . The state vector of the proposed UKF is constructed in equation (1)

$$x_k = [q_k, a_k^s, w_k^s, v_k, r_k] \quad (1)$$

Besides, the estimated acceleration and angular rate (a_k^s and w_k^s), the 15-element vector contains the attitude (q_k), and the velocity and position (v_k and r_k). All the these 5 components have 3 elements each, corresponding to a three-dimensional estimation.

The torch attitude is presented by a unit quaternion q_k , i.e., the attitude accounting for the angular rate w_k^s within one sampling time interval (Chou (1992)):

$$q_k = \exp(w_k^s * T_s/2) \quad (2)$$

where $\exp(\cdot)$ denotes the quaternion exponential:

$$\exp(v) = [\cos(\|v\|), v/\|v\| \times \sin(\|v\|)] \quad (3)$$

The quaternion at instant $k+1$ can be expressed using the quaternion at k instant:

$$q_{k+1} = q_k \otimes \exp(w_k^s * T_s/2) \quad (4)$$

where \otimes is the quaternion product defined as:

$$a \otimes b = [a_1 \ a_2 \ a_3 \ a_4] \otimes [b_1 \ b_2 \ b_3 \ b_4] = \begin{bmatrix} a_1 b_1 - a_2 b_2 - a_3 b_3 - a_4 b_4 \\ a_1 b_2 + a_2 b_1 + a_3 b_4 - a_4 b_3 \\ a_1 b_3 - a_2 b_4 + a_3 b_1 + a_4 b_2 \\ a_1 b_4 + a_2 b_3 - a_3 b_2 + a_4 b_1 \end{bmatrix}^T \quad (5)$$

Using a simplified model, the WIMU measurements are expressed in (6) and (7).

$$w_k^s = S_w w_{true,k}^s + T_w w_{true,k}^s + b_w + v_w \quad (6)$$

$$a_k^s = S_a a_{true,k}^s + T_a a_{true,k}^s + b_a + v_a \quad (7)$$

where $w_{true,k}^s$ and $a_{true,k}^s$ are the true value, S_w and S_a are the scale-factor matrices; T_w and T_a are the non-orthogonality factor matrices; b_w and b_a are the bias; and v_w and v_a are normally considered as uncorrelated white Gaussian noises, with a covariance matrix R .

The true acceleration measurement includes two components: the sensor acceleration and the gravitation acceleration, as expressed by Eq. 8.

$$a_{true,k}^s = a_{sensor,k}^s + g_k^s \quad (8)$$

where g_k^s is the gravitational acceleration in the sensor frame:

$$g_k^s = q_k \otimes [0, 0, 0, g] \otimes q_k^* \quad (9)$$

q_k^* is the transpose of q_k , and g is the local gravitation acceleration.

Since the acceleration of gravity is removed from the sensor readings, the velocity in the reference frame $v_{k|k-1}$, prior to the UKF correction at time:

$$v_{k|k-1} = v_{k-1|k-1} + a_{sensor,k}^s \cdot T_s \quad (10)$$

This velocity is integrated to obtain the torch position in the reference frame:

$$r_{k|k-1} = r_{k-1|k-1} + v_{k|k-1} \cdot T_s \quad (11)$$

To summary (4) to (11), the process model for the proposed UKF is:

$$x_{k+1} = f(x_k, \omega_k) \quad (12)$$

where $f(\cdot)$ contains equations from (4) to (11), and ω_k is the process noise with a covariance matrix denoted as Q_k .

The measurement model of the UKF can be written:

$$z_{k+1} = h(x_k, v_k) \quad (13)$$

where $z_{k+1} = [w_{k+1}^s, a_{k+1}^s]$, and $v_k = [v_w, v_a]$.

Because of the nonlinear nature of the process model, (12), and the sensor model, the UKF approach is applied (E.A.Wan and der Merwe (2000)). For the sake of readers' convenience, the UKF algorithm are summarized below.

Given the estimated state vector \hat{x}_{k-1} and its covariance P_{k-1} at instant $k-1$, an auxiliary vector set $\{\psi_i\}$ is defined by (14).

$$\psi_i = \begin{cases} \left(\sqrt{(n+\lambda) \cdot (P_{k-1} + Q)} \right)_i & i = 1, \dots, n \\ - \left(\sqrt{(n+\lambda) \cdot (P_{k-1} + Q)} \right)_{(i-n)} & i = n+1, \dots, 2n \end{cases} \quad (14)$$

where $\left(\sqrt{(n+\lambda) \cdot (P_{k-1} + Q)} \right)_i$ is the i^{th} row of the matrix square root, and $\lambda = \alpha^2(n+\kappa) - n$ in which α and κ are two scaling parameters.

UKF addresses the approximation of a nonlinear system by using a minimal set of sample points, i.e., sigma points, to capture the mean and covariance estimate. The sigma points set $\{(\chi_{k-1})_i\}$ is defined by

$$(\chi_{k-1})_i = \hat{x}_{k-1} \quad (15)$$

as $i = 0$, and

$$(\chi_{k-1})_i = \hat{x}_{k-1} + \psi_i \quad (16)$$

when $i = 1, \dots, 2n$, and $\psi_i = [\psi_{i|q}, \psi_{i|a}, \psi_{i|w}, \psi_{i|v}, \psi_{i|r}]$.

After the sigma points $\{(\chi_{k-1})_i\}$ are obtained, the process model is used to project each point ahead in time. The propagation results are shown in (17), and *a priori* state estimate is thus obtained in (18).

$$(\chi_k)_i = f((\chi_{k-1})_i, 0, 0) \quad \text{for } i = 0, \dots, 2n \quad (17)$$

$$\hat{x}_k^- = \sum_{i=0}^{2n} W_i^{(m)} (\chi_k)_i \quad (18)$$

where weights $W_i^{(m)}$ are defined by

$$W_i^{(m)} = \begin{cases} \lambda/(n+\lambda) & i = 0 \\ \lambda/(2(n+\lambda)) & i = 1, \dots, 2n \end{cases} \quad (19)$$

The covariance of $(\chi_k)_i$ is

$$P_k^- = \sum_{i=0}^{2n} W_i^{(c)} [(\chi_k)_i - \hat{x}_k^-]^T [(\chi_k)_i - \hat{x}_k^-] \quad (20)$$

where weights $W_i^{(c)}$ are defined in (21), β is a scaling parameter used to incorporate prior knowledge about the distribution of state vector x .

$$W_i^{(c)} = \begin{cases} \lambda/(n + \lambda) + (1 - \alpha^2 + \beta) & i = 0 \\ \lambda/(2(n + \lambda)) & i = 1, \dots, 2n \end{cases} \quad (21)$$

The results for the projected set $\{(\chi_k)_i\}$ in the sensor model are expressed by

$$(\mathbf{y}_k)_i = h((\chi_k)_i, 0, 0) \quad \text{for } i = 0, \dots, 2n \quad (22)$$

The measurement estimate can thus be defined in (23).

$$\hat{z}_k^- = \sum_{i=0}^{2n} W_i^{(m)} (\mathbf{y}_k)_i \quad (23)$$

The *a posteriori* state estimate is computed using

$$\hat{x}_k = \hat{x}_k^- + K_k (z_k - \hat{z}_k^-) \quad (24)$$

where z_k is the measurement vector from WIMU, and K_k is the Kalman gain which is defined by

$$K_k = P_{\hat{x}_k \hat{z}_k} P_{\hat{z}_k \hat{z}_k}^{-1} \quad (25)$$

The cross correlation matrix $P_{\hat{x}_k \hat{z}_k}$ and measurement estimate covariance $P_{\hat{z}_k \hat{z}_k}$ are expressed in (26) and (27), respectively.

$$P_{\hat{x}_k \hat{z}_k} = \sum_{i=0}^{2n} W_i^{(c)} [(\chi_k)_i - \hat{x}_k^-]^T [(\mathbf{y}_k)_i - \hat{z}_k^-] \quad (26)$$

$$P_{\hat{z}_k \hat{z}_k} = \sum_{i=0}^{2n} W_i^{(c)} [(\mathbf{y}_k)_i - \hat{z}_k^-]^T [(\mathbf{y}_k)_i - \hat{z}_k^-] + R \quad (27)$$

The estimated state covariance is updated at instant k by

$$P_k = P_k^- - K_k P_{\hat{z}_k \hat{z}_k} K_k^T \quad (28)$$

4. METHODS TO REDUCE SENSOR DRIFT

The attitude estimation of the torch can be corrected against the sensor bias in roll and pitch direction using the UKF in section III. However, the heading (yaw) drifting is uncontrolled. To this regard, the magnetometer reading is incorporated into the measurement model:

$$b_{k+1}^s = b_k^s + v_m = q_k \otimes [0, \mathbf{b}] \otimes q_k^* + v_m \quad (29)$$

where \mathbf{b} is the vector of the magnetic field ("north"), v_m is the measurement noise.

The Zero Velocity Update (ZUPT) and Zero Angular Rate Update (ZARU) can be implemented and integrated into the Kalman-based framework only when the torch stays

still during the welding process for a certain amount time. Three conditions to declare the torch as still are:

- (1) The magnitude of the acceleration, $\|a_k^s\|$, must be between to thresholds ($a_{min} = 9.5m/s^2$ and $a_{max} = 10.5m/s^2$):

$$a_{min} < \|a_k^s\| < a_{max} \quad (30)$$

- (2) The local acceleration variance, σ_{a_k} , must be below a given threshold ($\sigma_{max} = 0.5m/s^2$):

$$\sigma_{a_k} < \sigma_{max} \quad (31)$$

where

$$\sigma_{a_k}^2 = \frac{1}{2n+1} \sum_{j=k-n}^{k+n} (a_j^s - \bar{a}_j^s)^2 \quad (32)$$

where \bar{a}_j^s is a local mean acceleration value.

- (3) The magnitude of the gyroscope, $\|w_k^s\|$, must be below a given threshold ($w_{max} = 5^\circ/s$):

$$\|w_k^s\| < w_{max} \quad (33)$$

If the three conditions all holds, then ZUPT and ZARU are incorporated into the measurement model of the UKF methodology:

$$v_k = [0, 0, 0] \quad (34)$$

$$w_k^s = [0, 0, 0] \quad (35)$$

5. EXPERIMENTS AND RESULTS

We have conducted several tests in order to evaluate and compare the performances of Kalman-based INS algorithm, INS + magnetometer, and INS + magnetometer + ZUPT + ZARU. The WIMU mounted on the torch is shown in Fig. 1. Two kinds of experiment were conducted: 1) the torch was hold by a welder and smoothly moved along the 3 axes in a Cartesian coordinate system, as shown in Fig. 4, as it had been operated in a real welding act. Traveled distance $ox' = oy' = oz' = 300mm$; 2) the torch was smoothly moved along a 3-D trajectory as shown in Fig. 5, which is sine curve, $y = 150 \times \sin(2\pi/300)$, in a tilted plane (45° to the oxy plane). Traveled distance $oy' = 300mm$. The coordinate $y' = [0, 300, 300]mm$. For a valid application of ZUPT and ZARU, the torch randomly stopped for a very short time interval (around 100 ms) during the movement. The sampling time is 20 ms.

5.1 WIMU sensor

The size of the WIMU is about $53 \text{ mm} \times 32 \text{ mm} \times 19 \text{ mm}$, as shown in Fig. 1. It is an IMU with wireless capability which is composed of a tri-axial accelerometer (Freescale MMA7260Q), a tri-axial gyro sensor (InvenSense 500 series), a microprocessor (MSP430F1611), and a Bluetooth unit. The accelerometer is endowed with one filter capacitor in each axis. The gyro sensor contains three vibrating elements. The magnetometer uses a thin-film magnetoresistive principle to measure the earth magnetic field. The angular rate at each axis is obtained by measuring the Coriolis acceleration of the corresponding vibrating elements. The microprocessor captures the sensor data using

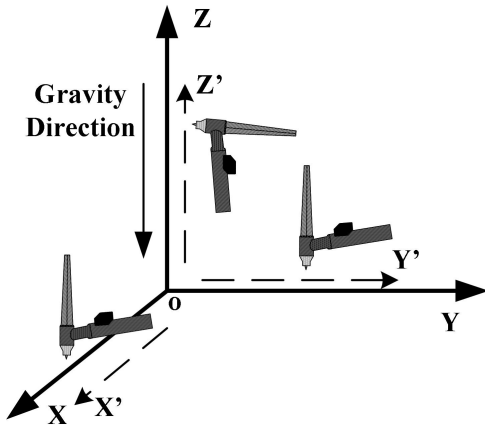


Fig. 4. Illustration of Experiment 1. The torch is smoothly moved along the three axes in the coordinate system.

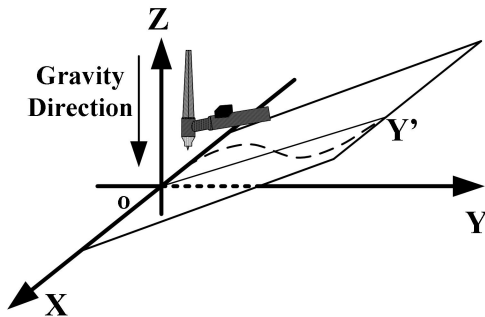


Fig. 5. Illustration of Experiment 2. The torch is smoothly moved along the 3-D sine curve.

a 12 bit analog-to-digital converter (ADC) at a pre-defined frequency. The Bluetooth unit transmits the data from the WIMU to a desktop.

5.2 UKF tuning

The Kalman-based framework had to be well-tuned in order to obtain a stable operation, by selecting the value of matrices Q_k , R_k and P_{k-1} . The results of the experiments strongly depend on the selected values for those covariance matrices, so the tuning process must be conducted such that a consistent response of the experiments can be acquired.

The process noise covariance matrix, Q_k , is initialized for $k=1$ as diagonal 15×15 matrix with the in-diagonal values: $[2 \times 10^{-4}, 0_{1 \times 3}, 0_{1 \times 3}, 1 \times 10^4, 0_{1 \times 3}]$.

The measurement noise covariance matrix R_k , is a $n \times n$ square diagonal matrix, while n is the number of measurement available. The settings are: 1×10^4 rad/s for gyroscope, $1 \times 10^2 mm/s^2$ for the acceleration, 0.1 rad for magnetometer, 0.001 m/s for ZUPT, and 0.1 rad/s for ZARU.

The state estimation covariance matrix, P_{k-1} , is initialized also as a diagonal matrix with the in-diagonal elements: $[0_{1 \times 3}, 1 \times 10^{-2}, 1 \times 10^2, 0_{1 \times 3}, 0_{1 \times 3}]$.

5.3 Experiment results

It was inevitable that the torch's trajectory in the experiments did not exactly coincide with the real trajectory since the torch was hold by a human. The deviation of position in direction other than the targeted direction/curve might indicate the human hand uncertainty in holding for a position due to the inherent neuro latency. The sampling and transmitting noise may also partially contribute to the deviations. The distance of the torch's movement has been carefully calibrated such that its actually traveled distance along the targeted direction/curve was accurate enough (position error $< 1 \times 10^{-2} mm$).

The torch was moved along the 3 axes of the shown in Fig. 4. The estimation results of the torch trajectory along the x-axis is shown in Fig. 6. It is clearly shown that with the drift reduction integrated in the Kalman-based INS algorithm, the position estimation accuracy is significantly improved.

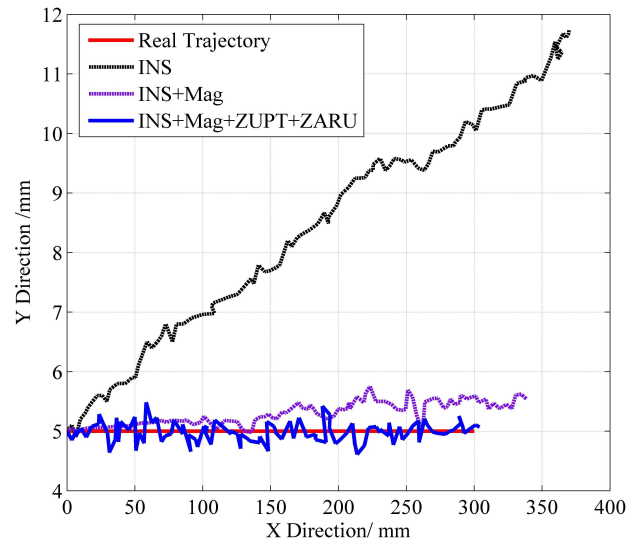


Fig. 6. The results of torch trajectory position estimation using different algorithms in Experiment 1.

Six trials were repeated for each direction of torch movement. The average measurement errors over the total traveled distance (TTD) are listed in table 1.

Table 1. Measurement errors in Experiment 1

Estimation methods	Position error (% of TTD)
Kalman-based INS	> 20
INS+magnetometer	[5-15]
INS+magnetometer+ZUPT+ZARU	[0.4-1.2]

Six trails were repeated for the second experiment as shown in Fig. 5. The estimation result in one trail is shown in Fig. 7.

The position measurement errors obtained from Experiment 2 using different estimation methodologies are listed in Table 2.

6. CONCLUSION

An innovative Kalman-based framework for torch's attitude and position measurement is developed in this paper.

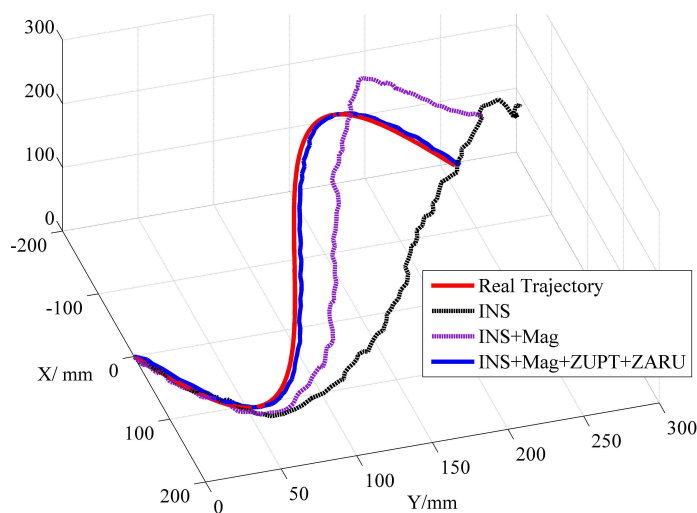


Fig. 7. The results of the torch trajectory position estimation using different algorithms in Experiment 2.

Table 2. Positioning errors in Experiment 2

Estimation methods	Position error (% of TTD)
Kalman-based INS	> 25
INS+magnetometer	[7-16]
INS+magnetometer+ZUPT+ZARU	[0.5-1.7]

Since the study is restricted to use an WIMU sensor alone, i.e., without using any external infrastructure such as GPS, LPS, or building-maps to correct the sensor drift. The proposed methodology can thus be conveniently adapted into an arc welding process or a welder training system.

The proposed methodology in this paper includes a Kalman-based INS algorithm with the integration of magnetometer, ZUPT and ZARU. The results verified the effectiveness of the proposed methodology. The position measurement error is typically about 1% of the total traveled distance.

Future work will be directed to utilize the proposed method to develop an innovative welding robot teaching and programming strategy.

ACKNOWLEDGEMENTS

This work is funded by the National Science Foundation under grant CMMI-0927707.

REFERENCES

(1997). Lincoln mig welding guidance. LINCOLN ELECTRIC, 22801 St. Clair Avenue, Cleveland, Ohio 44117-1199 USA.

(2003). Aws c5.5/c5.5m recommended practices for gas tungsten arc welding.

(2003). Guidelines to gas tungsten arc welding (gtaw). MILLER ELECTRIC.

(2004). Aws c5.6 recommended practices for gas metal arc welding.

(2011). *Welder Guide Book*. ESAB, P.O. Box 100545, 411 South Ebenezer Road, Florence, SC 29501-0545.

(2012). *VRTEX 360*. Lincoln Electric, Cleveland, Ohio 44117-1199 U.S.A, im10046-e edition.

Chou, J. (1992). Quaternion kinematic and dynamic differential equations. *IEEE Transactions on Robotics and Automation*, 8(1), 53–64.

E.A.Wan and der Merwe, R.V. (2000). The unscented kalman filter for nonlinear estimation. In *IEEE Adaptive Systems for Signal Processing, Communications, and Control Symposium*, 153 – 158.

Ferraris, F., Grimaldi, U., and Pavis, M. (1995). Procedure for effortless in-field. calibration of three-axis rate gyros and accelerometers. *Sensors and Materials*, 7, 311–330.

Lee, H.J. and Jung, S. (2009). Gyro sensor drift compensation by kalman filter to control a mobile inverted pendulum robot system. In *Industrial Technology, 2009. ICIT 2009. IEEE International Conference on*, 1–6.

Luinje, H.J. and Veltink, P.H. (2005). Measuring orientation of human body segments using miniature gyroscope and accelerometer. *Medical and Biological Engineering and Computing*, 43, 273–282.

Luinje, H. and Veltink, P. (2004). Inclination measurement of human movement using a 3-d accelerometer with autocalibration. *IEEE Transactions on Neural Systems and Rehabilitation Engineering*, 12(1), 112 – 121.

Moreno, P. (2013). *Welding Defects (1st ed.)*. Aracne.

Pham, T.M. (1992). Kalman filter mechanization for ins airstart. *IEEE AES System Magazine*, 7, 3–11.

Raj, B., Jayakumar, T., and Thavasimuthu, M. (2002). *Practical non-destructive testing*. Woodhead Publishing.

Rampaul, H. (2003). *Pipe welding procedures (2nd ed.)*. Industrial Press.

Schepers, H.M., Roetenberg, D., and Veltink, P.H. (2010). Ambulatory human motion tracking by fusion of inertial and magnetic sensing with adaptive actuation. *Medical & Biological Engineering & Computing*, 48(1), 27–37.

Teeravarunyou, S. and Poopatb, B. (2009). Computer based welding training system. *International Journal of Industrial Engineering*, 16(2), 116–125.